Chemical Engineering Journal 111 (2005) 205–211

Chemical Engineering Journal

www.elsevier.com/locate/cej

The role of wave propagation in hydrocyclone operations I: An axisymmetric streamfunction formulation for a conical hydrocyclone

E. Ovalle [a,*], R. Araya [b], F. Concha [a]

[a] *Department of Metallurgical Engineering, University of Concepción, Concepción, Chile*
[b] *Department of Mathematical Engineering, University of Concepción, Concepción, Chile*

Abstract

The objective of this work is to study the role of some wavelike motion observed in the interior of a conical hydrocyclone used in mineral processing operations. In this paper, we obtained a stable numerical solution of the equations of motion, using a streamfunction-vorticity formulation on non-structured mesh. The numerical solution is obtained in a finite element context, where a stabilization is imposed through an unusual finite element method (USFEM) scheme. Finally, an adaptive mesh refinement is used for to enhance the solution.

Keywords: Hydrocyclone; Streamfunction; Stabilized finite element

1. Introduction

Hydrocyclones are used widely in the chemical, mineral and powder-processing industries. They consist of a cylindrical section followed by a conical section, a central upper overflow tube (vortex finder) and a central lower discharge tube (apex). A suspension is introduced tangentially at the top of the cylindrical section causing a confined turbulent swirling motion with recirculation. In this centrifugal field, coarse and heavy particles move toward the wall and leave the hydrocyclone at the upper region, while the lighter leave through the apex.

The global behavior of the flow inside on a conical hydrocyclone is well known Kelsall [6] and several analytical and CFD calculation, for example, Bloor and Ingham [1] and Davidson [4], as well as laser Doppler measurement, Rajamani and Milin [13], have been done. The velocity profiles show that the intensity of the turbulent motion is maximum near the air core and walls and diminishes to the interior of the hydrocyclone.

In the operation of conical hydrocyclones, an outstanding feature is the undulatory and sometimes pulsating character of the air core, especially in the apex region during the transition between spray and roping. The air core is not static as shown by tomographic measurement (Williams et al. [14]), and some capillary waves on the free surface exist as suggested by Dyakowski et al. [5]. Furthermore, some experimental evidence of the degradation of classification efficiency by instabilities has been reported by Luo et al. [11]. The objective of this study is to analyze the effect of the presence of waves (at the air core and in the interior of a hydrocyclone) on the classification action of the hydrocyclone and on the initiation of roping. Toward this goal, we combine laser Doppler anemometry measurements with numerical computations.

The work is organized in two parts. The first part, corresponding to this paper, is the solution of the Navier–Stokes equations in a hydrocyclone using a streamfunction-vorticity formulation in a finite element scheme. We apply an unusual FEM scheme, due to Franca and Valentin [7], for the treatment of numerical instabilities produced by the equations of motion in the form of convection–diffusion equations. The solution is enhanced by the use of adaptive meshes. The second part of the presented paper deals with the analysis of the wave propagation at the air–water interface of a hydrocyclone and the study of the effect of the waves in the hydrocyclone performance.

* Corresponding author.

1385-8947/$ – see front matter © 2005 Published by Elsevier B.V.
doi:10.1016/j.cej.2005.02.009

Nomenclature

C_h	finite element partition of Ω
p	pressure
Pe	Peclet number
r	radial coordinate
Re	Reynolds number
u	radial velocity
v	tangential velocity
w	axial velocity
z	axial coordinate

Greek letters

β	reduced vorticity
Γ	circulation
η	vorticity
ν	laminar viscosity
Ω	domain
ψ	stream function

2. The model

The flow of a hydrocyclone is assumed to have axisymmetrical character of the velocity field (except in the entrance region); therefore, we use cylindrical coordinates (r, ϕ, z), where the velocity field is $\boldsymbol{v} \equiv (u, v, w)$ and the pressure is p. The continuity and Navier–Stokes equations are

$$\nabla \cdot \boldsymbol{v} = 0 \tag{1}$$

$$\frac{\mathrm{D}\boldsymbol{v}}{\mathrm{D}t} = -\frac{1}{\rho}\nabla p + \nu \nabla^2 \boldsymbol{v} \tag{2}$$

Since the flow is two-dimensional, it is convenient to use a streamfunction-vorticity formulation instead of equation (2)

$$\frac{\mathrm{D}\boldsymbol{w}}{\mathrm{D}t} = \boldsymbol{w} \cdot \nabla \boldsymbol{v} + \nu \nabla^2 \boldsymbol{w} \tag{3}$$

where the components of the vorticity vector $\boldsymbol{w} = \nabla \times \boldsymbol{v} \equiv (\xi, \eta, \zeta)$ are

$$\xi = -\frac{\partial v}{\partial z}; \qquad \eta = \frac{\partial u}{\partial z} - \frac{\partial w}{\partial r}; \qquad \zeta = \frac{1}{r}\frac{\partial}{\partial r}(rv) \tag{4}$$

Then, in terms of components, equation (3) is given by

$$\frac{\mathrm{D}\xi}{\mathrm{D}t} = \xi\frac{\partial u}{\partial r} - \frac{v\eta}{r} + \zeta\frac{\partial u}{\partial z} + \nu\left[\frac{\partial}{\partial r}\left(\frac{1}{r}\frac{\partial}{\partial r}(r\xi)\right) + \frac{\partial^2 \xi}{\partial z^2}\right] \tag{5}$$

$$\frac{\mathrm{D}\eta}{\mathrm{D}t} = \xi\frac{\partial v}{\partial r} - \frac{u\eta}{r} + \zeta\frac{\partial v}{\partial z} + \nu\left[\frac{\partial}{\partial r}\left(\frac{1}{r}\frac{\partial}{\partial r}(r\eta)\right) + \frac{\partial^2 \eta}{\partial z^2}\right] \tag{6}$$

$$\frac{\mathrm{D}\zeta}{\mathrm{D}t} = \xi\frac{\partial w}{\partial r} + \zeta\frac{\partial w}{\partial z} + \nu\left(\frac{\partial^2 \zeta}{\partial r^2} + \frac{1}{r}\frac{\partial \zeta}{\partial r} + \frac{\partial^2 \xi}{\partial z^2}\right) \tag{7}$$

If the velocities are expressed in terms of the streamfunction, ψ, such that $u = -\frac{1}{r}\frac{\partial \psi}{\partial z}$ and $w = \frac{1}{r}\frac{\partial \psi}{\partial r}$, equation (6) is

$$\frac{\partial \eta}{\partial t} = \frac{1}{r^3}\frac{\partial \Gamma^2}{\partial z} + \frac{u\eta}{r} - u\frac{\partial \eta}{\partial r} - w\frac{\partial \eta}{\partial z} + \nu\left[\frac{\partial}{\partial r}\left(\frac{1}{r}\frac{\partial}{\partial r}(r\eta)\right) + \frac{\partial^2 \eta}{\partial z^2}\right] \tag{8}$$

and v component of equation (1) can be written in terms of the circulation, $\Gamma = vr$, as

$$\frac{\partial \Gamma}{\partial t} = -u\frac{\partial \Gamma}{\partial r} - w\frac{\partial \Gamma}{\partial z} + \nu\left[r\frac{\partial}{\partial r}\left(\frac{1}{r}\frac{\partial \Gamma}{\partial r}\right) + \frac{\partial^2 \Gamma}{\partial z^2}\right] \tag{9}$$

with η given by

$$\eta = -\frac{\partial}{\partial r}\left(\frac{1}{r}\frac{\partial \psi}{\partial r}\right) - \frac{1}{r}\frac{\partial^2 \psi}{\partial z^2} \tag{10}$$

The Reynolds number, Re, can be related to the viscosity in terms of the mean entrance velocity $\bar{U}_0$ and the hydrocyclone radius $\bar{R}_c$. We introduce some normalization constants; Hsieh [10] defined, in terms of the old (barred) and new dimensionless variables (non-barred), by $t = \bar{t}/(\bar{R}_c/\bar{U}_0)$, $r = \bar{r}/\bar{R}_c$, $z = \bar{z}/\bar{R}_c$, $u = \bar{u}/\bar{U}_0$, $\Gamma = \bar{\Gamma}/(\bar{U}_0\bar{R}_c)$, $w = \bar{w}/\bar{U}_0$, $\eta = \bar{\eta}/(\bar{U}_0/\bar{R}_c)$, $\psi = \bar{\psi}/(\bar{R}_c^2\bar{U}_0)$, the new equations for η and Γ conserve the same form, but now the viscosity can be expressed in terms of the Reynolds number $\nu \equiv 1/Re$ with $Re = \bar{R}_c\bar{U}_0/\bar{\nu}$.

It is possible to write equation (8) for η in the form of convection–diffusion equation also, if we use the new variable $\beta = \eta/r$. Then,

$$\frac{\partial \beta}{\partial t} + u\frac{\partial \beta}{\partial r} + w\frac{\partial \beta}{\partial z} = \nu\left[\frac{1}{r}\frac{\partial}{\partial r}\left(r\frac{\partial \beta}{\partial r}\right) + \frac{2}{r}\frac{\partial \beta}{\partial r} + \frac{\partial^2 \beta}{\partial z^2}\right] + \frac{\partial}{\partial z}\left(\frac{\Gamma^2}{r^4}\right) \tag{11}$$

In general, equations that include convection terms are difficult for solve. It is well known, for example, that for $\frac{\nu}{|\boldsymbol{v}|h} \ll \mathrm{O}(1)$, the standard numerical methods (central finite difference scheme and Galerkin formulation) lose stability manifested by large node-to-node fluctuations in the approximate solutions.

A great deal of mathematical and scientific research has been devoted to rectifying this problem. These methods generally try to remain true to the governing equations while simultaneously providing numerical stability to the solution. One of the simplest (yet effective) methods for obtaining stability is by the addition of artificial diffusion throughout the domain of the problem. In the next section, we present a finite element solution for η and β, using a stabilized method.

3. The finite element solution

3.1. The numerical scheme

In comparison to the numerical solution to the equations of motion obtained by Hsieh and Rajamani [9], which uses a finite difference scheme, in this work, we present a solution using a finite element formulation. In an FEM formulation, the application of boundary conditions and the utilization of more complex non-structured grids are advantageous.

When using standard Galerkin methods, the convection–diffusion equation is difficult to solve for high Peclet numbers (see equation (28)). Strong oscillations occur in regions of higher gradient of the hydrodynamical fields. In order to improve the Galerkin solution, two successful stabilized methods have been used: the streamline upwinding Petrov Galerkin (SUPG) methods [3] and the residual-free-bubbles methods [8]. In particular, the SUPG method adds numerical diffusion along the streamline direction, damping the oscillations.

In this paper, we will use the unusual finite element method (USFEM) technique on triangular grids [7], since it produces less diffusion that the standard SUPG methods. This technique combines the residual-free-bubbles methods with standard Petrov Galerkin methods. Before applying the FEM to solve the equations, it is necessary to transform the equations into more suitable forms. To do that, there are two alternatives: one can derive an equivalent minimization problem, which has exactly the same solution as the differential equation, or one can derive a so-called weak formulation. Originally, the weak formulation was introduced by mathematicians to investigate the behavior of the solution of partial differential equations, and to prove existence and uniqueness of the solution. Later on, numerical schemes were based on this formulation, which lead to an approximate solution in a constructive way.

Consider a differential operator, $\mathcal{L}$, and C_h, a finite element partition of Ω, made up with three nodes triangles. If we write the differential equation in the form

$$\mathcal{L}u = f, \tag{12}$$

we replace the variational for $(\mathcal{L}u, v) = (f, v)$ by the stabilized formulation

$$(\mathcal{L}u, v) - \sum_{K \in C_h} (\mathcal{L}u, \tau\mathcal{L}^\dagger v)_K = (f, v) - \sum_{K \in C_h} (f, \tau\mathcal{L}^\dagger v)_K \tag{13}$$

where $\mathcal{L}^\dagger$ is a discrete adjunct operator to $\mathcal{L}$, $(\cdot,\cdot)_K$ is a discrete inner product that, in the continuous version, is

$$(\mathcal{L}u, v) = \int_\Omega \mathcal{L}(u)v \,\mathrm{d}\Omega = \int_\Omega u\mathcal{L}^\dagger(v) \,\mathrm{d}\Omega = (u, \mathcal{L}^\dagger v) \tag{14}$$

and τ is a parameter depending on the element K of C_h and some local Peclet number. In (14), the terms that produce the stabilization contain functions that belong to the discrete space $V_h \subset H_0^1(\Omega)$.

In our case, the two convection–diffusion models considered can be written as the following boundary value problem:

$$\frac{\partial \Gamma}{\partial t} + \boldsymbol{a} \cdot \nabla\Gamma - \nu\left(\nabla^2\Gamma - \frac{1}{r}\frac{\partial \Gamma}{\partial r}\right) = 0 \text{ in } \Omega \tag{15}$$

$$\frac{\partial \beta}{\partial t} + \boldsymbol{a} \cdot \nabla\beta - \nu\left(\nabla^2\beta - \frac{3}{r}\frac{\partial \beta}{\partial r}\right) = f^{(\beta)} \text{ in } \Omega \tag{16}$$

where $\boldsymbol{a} \equiv (u, w)$ is the given velocity field, $\nabla \equiv \left(\frac{\partial}{\partial r}, \frac{\partial}{\partial z}\right)$ and $\nabla^2 \equiv \left(\frac{\partial^2}{\partial r^2}, \frac{\partial^2}{\partial z^2}\right)$ are gradient and Laplacian Cartesian operators. Furthermore, the source term of (16) is $f^{(\beta)} \equiv \frac{\partial}{\partial z}\left(\frac{\Gamma^2}{r^4}\right)$. For the treatment of the variational form of these equations, it is necessary to work with an internal product defined by

$$(u, v) \equiv \int_\Omega uv \,\mathrm{d}\Omega \tag{17}$$

with $\mathrm{d}\Omega = r\,\mathrm{d}r\,\mathrm{d}z$ that corresponds to an internal product in cylindrical coordinates. Consider a space $H_0^1(\Omega)$ of continuous functions with continuous first derivative in a bounded domain $\Omega \subset R^2$ and null Neumann conditions at the boundary $\partial\Omega$. The variational formulation corresponding to (15) is: find $u \in H_0^1(\Omega)$, such that $\forall v \in H_0^1(\Omega)$

$$(\dot{u}, v) + (\boldsymbol{a} \cdot \nabla u, v) - \nu(\nabla^2 u, v) + \nu\left(\frac{1}{r}\frac{\partial u}{\partial r}, v\right) = 0 \tag{18}$$

Similarly, for (16) it is: find $u \in H_0^1(\Omega)$, such that $\forall v \in H_0^1(\Omega)$

$$(\dot{u}, v) + (\boldsymbol{a} \cdot \nabla u, v) - \nu(\nabla^2 u, v) - 3\nu\left(\frac{1}{r}\frac{\partial u}{\partial r}, v\right) = (f^{(\beta)}, v) \tag{19}$$

The standard Galerkin method consists in choosing a finite dimensional sub-space, $V_h \subset H_0^1(\Omega)$, and solving the following: for Γ, find $u_h \in V_h$, such that $\forall v_h \in V_h(\Omega)$

$$(\dot{u}_h, v_h) + (\boldsymbol{a} \cdot \nabla u_h, v_h) - \nu(\nabla^2 u_h, v_h) - \nu\left(\frac{1}{r}\frac{\partial u_h}{\partial r}, v_h\right) = 0 \tag{20}$$

and for β, find $u_h \in V_h$, such that $\forall v_h \in V_h(\Omega)$

$$(\dot{u}_h, v_h) + (\boldsymbol{a} \cdot \nabla u_h, v_h) - \nu(\nabla^2 u_h, v_h) - 3\nu\left(\frac{1}{r}\frac{\partial u_h}{\partial r}, v_h\right) = (f^{(\beta)}, v_h) \tag{21}$$

It is well known that for a subspace spanned by piecewise linear elements, these formulations yield poor approximations when $\nu \ll |\boldsymbol{a}|$. In this paper, we propose to apply an extension to the unusual stabilized method introduced in [7] to problems in cylindrical coordinates. The method can be written as:

For the equation for Γ: find $u_h \in V_h$, such that

$$(\dot{u}_h, v_h) + B(u_h, v_h) = 0, \quad \forall v_h \in V_h \tag{22}$$

where

$$B(u,v) = (\boldsymbol{a}\cdot\nabla u, v) + \nu(\nabla u, \nabla v) + 2\nu\left(\frac{1}{r}\frac{\partial u}{\partial r}, v\right) + \sum_{K\in C_h}\left(\boldsymbol{a}\cdot\nabla u - \nu\,\Delta u + \frac{\nu}{r}\frac{\partial u}{\partial r}, \tau_K \times \left(\boldsymbol{a}\cdot\nabla v + \nu\,\Delta v + \frac{3\nu}{r}\frac{\partial v}{\partial r} + \frac{a_r v}{r}\right)\right)_K \quad (23)$$

and for the equation for β: find $u_h \in V_h$, such that

$$(\dot{u}_h, v_h) + B(u_h, v_h) = F(v_h), \quad \forall v_h \in V_h \quad (24)$$

where

$$B(u,v) = (\boldsymbol{a}\cdot\nabla u, v) + \nu(\nabla u, \nabla v) - 2\nu\left(\frac{1}{r}\frac{\partial u}{\partial r}, v\right) + \sum_{K\in C_h}\left(\boldsymbol{a}\cdot\nabla u + \nu\,\Delta u - \frac{3\nu}{r}\frac{\partial u}{\partial r}, \tau_K \times \left(\boldsymbol{a}\cdot\nabla v + \nu\,\Delta v - \frac{\nu}{r}\frac{\partial v}{\partial r} + \frac{a_r v}{r}\right)\right)_K \quad (25)$$

and

$$F(v) = (f^{(\beta)}, v) + \sum_{K\in C_h}\left(f^{(\beta)}, \tau_K\left(\boldsymbol{a}\cdot\nabla v + \nu\,\Delta v - \frac{v}{r}\frac{\partial v}{\partial r} + \frac{a_r v}{r}\right)\right)_K \quad (26)$$

As is shown in [7], the stability parameter can be chosen as

$$\tau_K = \frac{h_K^2}{6\nu\,\max\{Pe_K(\boldsymbol{x}), 1\}} \quad (27)$$

where

$$Pe_K(\boldsymbol{x}) = \frac{3|\boldsymbol{a}(\boldsymbol{x})|_2 h_K}{\nu} \quad (28)$$

$$|\boldsymbol{a}(\boldsymbol{x})| = \left(\sum_{i=1}^{N}|a_i(\boldsymbol{x})|^2\right)^{1/2} \quad (29)$$

The formula for τ_K has a form that is suggested by static condensation, as explained in [8].

We finalize this section by writing a variational form for the ψ equation given in (10), but now in terms of the reduced vorticity β

$$\beta r^2 = -\frac{\partial^2\psi}{\partial r^2} - \frac{\partial^2\psi}{\partial z^2} + \frac{1}{r}\frac{\partial\psi}{\partial r} \quad (30)$$

in the variational form: for β and ψ, find $v_h \in H_0^1$, such that

$$(\beta r^2, v) = (\nabla\psi, \nabla v) + 2\left(\frac{1}{r}\frac{\partial\psi}{\partial r}, v\right) \quad (31)$$

3.2. The integration in time

For integration in time, we use the implicit scheme because it is unconditionally stable scheme. If for an arbitrary field ϕ, the equation that we want to solve has the general form

$$[A]\dot{\phi} + [B]\phi = [F] \quad (32)$$

then, the solution is

$$\phi^{t+\Delta t} = ([A] + \Delta t[B])^{-1}([A]\phi^t + [F]\,\Delta t) \quad (33)$$

4. The boundary conditions

4.1. Inlet

Since ψ is not a function of v at the inlet region, we assign a turbulent velocity profile represented by a constant function

$$u_{in} = -\frac{1}{r_{in}}\frac{\partial\psi}{\partial z} \quad (34)$$

Integrating this function, we obtain a profile for the stream-function at $r = r_{in}$. While the velocity profile is axisymmetric with respect to z_0, ψ is antisymmetric. The inlet flow is proportional to the difference of the extreme values of ψ over the inlet region. We can set a constant value of ψ over the total upper wall of hydrocyclone $\psi_b = \psi(r_{in}, z_2)$. Similarly, $\psi_a = \psi(r_{in}, z_1)$ over the walls that contains the conical mantle of the hydrocyclone.

Since the vorticity can be calculated explicitly in term of the velocities, u and w, in the form $\eta = \partial u/\partial z - \partial w/\partial r$, the calculation of η in the inlet region is direct if we suppose that the tangential velocity, w, has no radial component.

The circulation, Γ, is proportional to the tangential velocity v; therefore, it can be defined in the form $\Gamma_{in} = v_{in}/R$, where v_{in} represents the tangential velocity field induced inside the hydrocyclone. Writing the axisymmetric approximation, we can calculate v_{in}. In the following form, we assume that a volume flow $Q_{in} = Q_o + Q_u$ is fed into the hydrocyclone through a pipe of radius, R_{in}, with a transversal section, $A_{in} = \pi R_{in}^2$. Then, the velocity modulus is given by $v_s \equiv |\boldsymbol{v}| = Q_{in}/A_{in}$, and the entrance velocity can be split into radial and tangential components. The radial component is calculated as $u_{in} = Q_{in}/(2\pi r_{in}\,\Delta z)$, while the tangential is $w_{in} = \sqrt{v_s^2 - u_{in}^2}$.

4.2. Walls

At the wall in the top section of the hydrocyclone, we set the values of the streamline function to the constant value of $\psi_b = \psi(r_{in}, z_2)$. Similarly, we set $\psi_a = \psi(r_{in}, z_1)$ at the conical wall. The vorticity can be calculated explicitly in terms of the velocities, u and w, in the form $\eta = \partial u/\partial z - \partial w/\partial r$. Finally,

the circulation we can be written $\Gamma_{\text{wall}} = kv_{\text{in}}/r$, where k is a constant factor. This fact is supported by the experimental evidence that the tangential velocity is not zero near the walls.

4.3. Free surface

The free surface has a behavior similar to a wall except free slip occurs, because there is no significant friction between the liquid and gas phases at the interface. Therefore, ψ can be considered constant at the free surface, say ψ_{fs}. This constant has a value between that of the walls that limit the inlet region, $\psi_{\text{o}} \leq \psi_{\text{fs}} \leq \psi_{\text{u}} \cdot \psi_{\text{o}}$ is the value of ψ_{u} over the upper section of the hydrocyclone and ψ_{o} is the value on the cylindrical and conical walls. The exact value of ψ_{fs} will depend, of course, on the flow split $f \equiv Q_{\text{o}}/Q_{\text{u}}$, where Q_{o} and Q_{u} are the overflow and underflow volume rates. The difference in the values of ψ on two different streamlines is equal to the volume rate of fluid between them (divided by 2π in the cylindrical case). Then,

$$f = \frac{\psi_{\text{o}} - \psi_{\text{fs}}}{\psi_{\text{fs}} - \psi_{\text{u}}} \tag{35}$$

Since the free surface is like a wall, the tangential velocity is not zero and we can write $\Gamma_{\text{fs}} = kv_{\text{in}}/r$ in the same form as was discussed before.

4.4. Outlets

At the outlet regions (over and underflow), we impose the usual boundary condition of constant fields in the $\hat{n}$ direction, that is $\frac{\partial \psi}{\partial n} = 0$, $\frac{\partial \eta}{\partial n} = 0$ and $\frac{\partial \Gamma}{\partial n} = 0$, where n is the normal unit vector at the outlet surfaces. The choice is consistent with the more general boundary conditions applied for the velocity fields $\frac{\partial u}{\partial z} = -\frac{1}{r}\frac{\partial^2 \psi}{\partial z^2}$ and $\frac{\partial w}{\partial n} = \frac{1}{r}\frac{\partial^2 \psi}{\partial z \partial r} = 0$, if $\frac{\partial \psi}{\partial n} = \frac{\partial \psi}{\partial z} = 0$. In this formulation, the boundary conditions on outlet regions are null Neumann boundary conditions and the superficial integrals are zero.

4.5. Dirichlet boundaries

In general, the Dirichlet boundary conditions can be applied as follows: suppose that we need to solve an equation of the form $[A]\{\psi\} = \{B\}$, where $[A]$ is a $n \times n$ matrix and $\{\psi\}$ with $\{B\}$ are vectors of $n \times 1$ dimension. If ψ is known over m nodes belonging to the contour Γ, but not over the $n - m$ belonging to $\tilde{\Omega} \equiv \Omega - \Gamma$, we can split the vectorial space for ψ, into two disjoint subspaces ψ_Γ and $\psi_{\tilde{\Omega}}$ in the form

$$\begin{bmatrix} A_{\Gamma\Gamma} & A_{\Gamma\tilde{\Omega}} \\ A_{\tilde{\Omega}\Gamma} & A_{\tilde{\Omega}\tilde{\Omega}} \end{bmatrix} \begin{Bmatrix} \psi_\Gamma \\ \psi_{\tilde{\Omega}} \end{Bmatrix} = \begin{Bmatrix} B_\Gamma \\ B_{\tilde{\Omega}} \end{Bmatrix} \tag{36}$$

and the solution for $\psi_{\tilde{\Omega}}$ is given by

$$\psi_{\tilde{\Omega}} = A^{-1}_{\tilde{\Omega}\tilde{\Omega}}(B_{\tilde{\Omega}} - A_{\tilde{\Omega}\Gamma}\psi_{\tilde{\Omega}}). \tag{37}$$

5. Results

The computational flow diagram used can be described in the following steps: at time $t = t_0$, the variable, ψ, is fixed in the Dirichlet boundaries and then are solved assuming that they satisfy Laplace's equation. We need a smooth field ψ for the calculations of the velocities, u and w. Now, we calculate the new values of the reduced vorticity, β, and the circulation, Γ, using the evolution equations (22) and (24) for a time $t = t_0 + \Delta t$. Then, we recalculate the streamfunction, ψ, using (31), the velocity fields u and w, and the new values for the boundaries of β. The cycle is repeated for $t = t + \Delta t$ until the fields do not change significantly in time.

Our calculations were based on a hydrocyclone with dimensions equal to those used by Rajamani and co-workers [12], which are given in Table 1. In general, the solution reproduces observations seen in the experiments for the velocity fields, as well as the recirculation near the entrance zone. The locus of zero axial velocity is also shown to occur. Strictly, it is not possible to obtain a numerical solution with only one computational run, because the outlets' areas and the split ratio of the flow for a given feed area are not known in advance. A series of calculations is needed to choose a solution that takes some functional to an extreme, for example, the total pressure drop. Fig. 1 shows a comparison between the measurement by Rajamani and co-workers [12] and one of our calculations for the flow split and for the outlet areas given in Table 1, and the tangential velocity profile.

When a stabilization scheme is not applied, some field, such as the vorticity and the velocities, present non-physical oscillations. This occurs for the streamfunction (see Fig. 2 for the results obtained with and without stabilization). If laminar flow is solved, the calculated tangential velocity has generally the form, of a free vortex. To reproduce the Rankine form, typical of the tangential velocity field in a hydrocyclone, it is necessary to introduce an additional viscosity at the inner region of hydrocyclone, near the air core. This is achieved by using a turbulence model. In our case, we use a simple Prandtl mixed-length model, designed specially for the flow in he

Table 1
Hydrocyclone Krebs

Dimension (mm)	
Diameter hydrocyclone	75.00
Longitude cylindrical region	75.00
Feed diameter	25.00
Vortex finder length	50.00
Cylindrical section length	75.00
Conical section length	185.0
Spigot diameter	12.5
Operation variables (kg/min)	
Feed flux	67.00
Underflow	14.34
Outlet areas (m^{-3})	
Overflow	4.4×10^{-3}
Underflow	9.44×10^{-5}

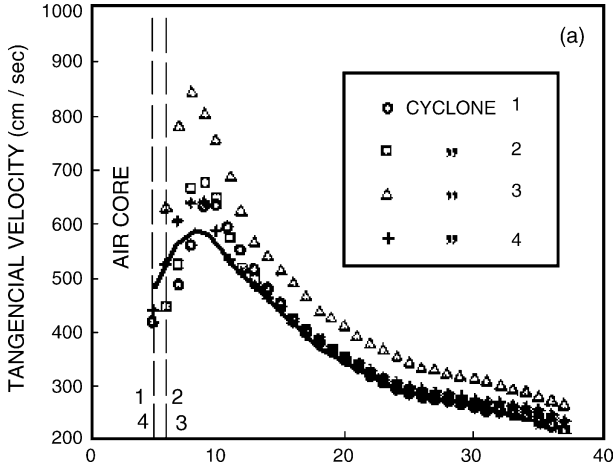

Fig. 1. Tangential velocity profile at level $z = 50$ mm from top in Ref. [12]. Each symbol corresponds to different operating conditions given in Table 2 in the paper. The operating condition chosen is shown with the symbol (□) (case 2 in paper). The line corresponds to the calculated profile in the present work.

hydrocyclone (Hsieh and Rajamani [9]). If μ is the dynamic viscosity of the fluid, this model adds a turbulent viscosity μ_t, expressed in terms both the gradients of velocity fields and of an empirical modulation induced by the geometry of the hydrocyclone.

$$\mu_t = K(R_c, \rho, \lambda(z, r), \mu_0) \left(\left| \frac{1}{r} \frac{\partial \Gamma}{\partial r} - \frac{2\Gamma}{r^2} \right| + \left| \frac{\partial w}{\partial r} \right| \right) \quad (38)$$

In (38), R_c is the hydrocyclone radio, ρ the density, μ_0 the fluid viscosity and $\lambda(z, r)$ is defined as an empirical function. In our case, we use $K = 5 \times 10^{-4}$. The calculations were made in Matlab, and a mesh generator BL2D [2] was used for the construction of an adaptive mesh. Fig. 3 shows the initial and final meshes used. The last mesh contains 1109 points and 1987 triangles. The time step used was 0.0025 s and the resulting Reynolds number was $Re = 8.53 \times 10^4$.

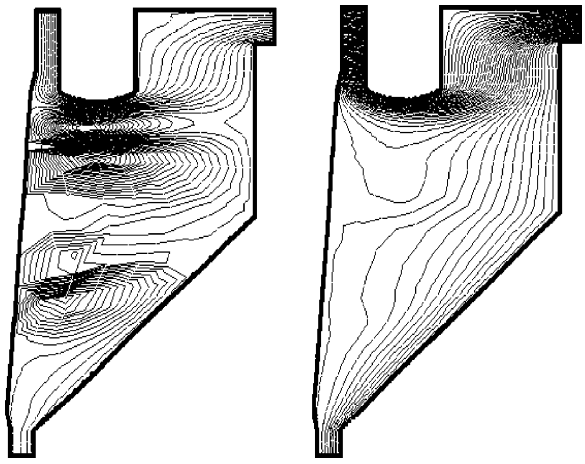

Fig. 2. Streamfunction solution with and without stabilization scheme.

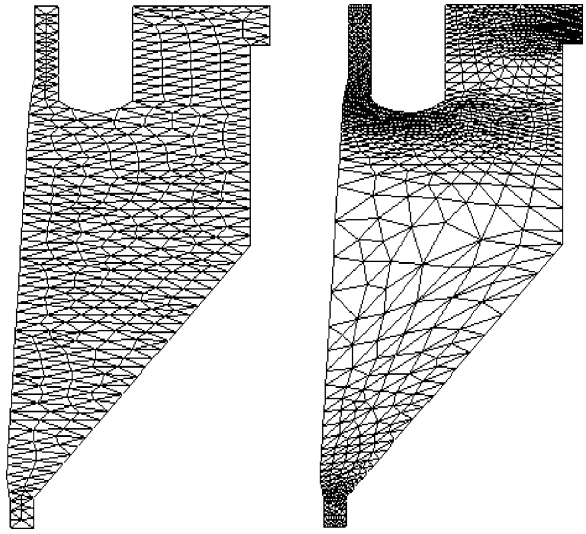

Fig. 3. Initial and adapted meshes.

6. Conclusions

A stabilized solution for the equations of motion that govern the dynamics of a conical hydrocyclone has been developed, using a USFEM scheme in a finite element formulation. The advantages over finite differences formulations are in the application of boundary conditions (especially in the outlet regions) and in the use of non-structured meshes that permits the generation of adaptive meshes to enhance the solution in zones where there is a greater change in the field.

The presented stabilized method achieves a numerical solution even in the case when we use a laminar viscosity. In this case, a free-vortex profile for the tangential velocity is obtained. The adjustment of the experimental form of a Rankine profile is obtained through a turbulence model. In particular, a simple Prandtl turbulence model is sufficient to obtain a good solution in a triangular mesh.

Acknowledgements

We acknowledge financial support from the following projects: Fondecyt N298005, Fondef MI-08 and F-1064 and from the Graduate School and Research Council at the University of Concepción.

References

[1] M.I.G. Bloor, D.B. Ingham, Theoretical investigations of the flow in a conical hydrocyclone, Trans. Inst. Chem. Eng. 51 (1973) 36–41.
[2] H. Borouchaki, P. Laug, Le mailleur adaptif bidimensionnel BL2D: Manuel d'utilisation et documentation, Rapport Tecchique INRIA RT-0195 (1995).
[3] A.N. Brooks, T.J.R. Hughes, Streamline upwind/Petrov–Galerkin formulations for convection dominated flows with particular emphasis on the incompressible Navier–Stokes equations, Comput. Methods Appl. Mech. Eng. 32 (1982) 199–259.

[4] M. Davidson, Similarity solutions for flow in hydrocy clones, Chem. Eng. Sci. 43 (7) (1988) 1499.
[5] T. Dyakowski, G. Hornung, R.A. Williams, Simulation of non-Newtonian flow in a hydrocyclone, Trans. IChemE 72 (Part A) (1994) 513–520.
[6] D.F. Kelsall, A study of the motion of solid particles in a hydraulic cyclone, Trans. Inst. Chem. Eng. 30 (1952) 87–108.
[7] L.P. Franca, F. Valentin, On an improved unusual stabilized finite element method for the advective–reactive–diffusive equation, Comput. Methods Appl. Mech. Eng. 190 (2000) 1785–1800.
[8] L.P. Franca, C. Farhat, Bubble functions prompt unusual stabilized finite element methods, Comput. Methods Appl. Mech. Eng. 156 (1995) 185–210.
[9] T.K. Hsieh, K.T. Rajamani, Phenomenological model of the hydrocyclone: model development and verification for single phase flow, Int. J. Miner. Process. 22 (1988) 223–237.
[10] T.K. Hsieh, Phenomenological model of the hydrocyclone, Ph.D. Thesis, University of Utah, Salt Lake City, 1988 (UT 84112).
[11] Q. Luo, C. Deng, J. Xu, L. Yu, G. Xiong, Comparison of the performance of water-sealed and commercial hydrocyclones, Int. J. Miner. Process. 25 (1989) 297–310.
[12] T.C. Monderon, K.T. Hsieh, R.K. Rajamani, Fluid flow model of the hydrocyclone: an investigation of device dimensions, Int. J. Miner. Process. 35 (1992) 65–83.
[13] R. Rajamani, L. Milin, Fluid flow model of the hydrocyclone for concentrated slurry classification, in: 4th International Conference on Hydrocyclones, Southhampton, England, 1992, p. 95.
[14] R. Williams, O. Ilyas, T. Dyakowski, Air core imaging in cyclone coal separator using electrical resistance tomography, Coal Prep. 15 (1995) 143–163.